Molecular Orientation Distributions in Protein Films. 1. Cytochrome *c* Adsorbed to Substrates of Variable Surface Chemistry

Paul L. Edmiston, John E. Lee, Shih-Song Cheng, and S. Scott Saavedra*

Contribution from the Department of Chemistry, University of Arizona, Tucson, Arizona 85721

Received July 10, 1996. Revised Manuscript Received November 5, 1996[⊗]

Abstract: Molecular orientation in hydrated cytochrome *c* (cyt *c*) films formed by adsorption to substrates of differing surface chemistry was investigated. The orientation distribution of the heme groups in the protein films was determined using a combination of two techniques: absorption linear dichroism, measured in a planar integrated optical waveguide-attenuated total reflection geometry, and emission anisotropy, measured in a total internal reflection fluorescence geometry. The mean heme tilt angle and angular distribution about the mean were recovered using a Gaussian model for the orientation distribution. These data are the first orientation distribution measurements reported for protein film assemblies. The results show that a macroscopically ordered film of adsorbed cyt *c* molecules is produced when a single, high-affinity type of noncovalent binding occurs between the surface of the protein and the substrate surface. For example, electrostatic adsorption of the positively charged protein to the negatively charged head groups of a Langmuir−Blodgett film of arachidic acid produces a narrow orientation distribution. When multiple, competing adsorptive interactions are operative, which is the case when cyt *c* adsorbs to a clean glass surface, a relatively disordered film is produced.

Introduction

Due to their large size and chemically heterogeneous nature, proteins are highly surface active molecules. Thus, an adsorbed protein film will form when a solution of dissolved proteins contacts the surface of virtually any synthetic material.[1,2] Understanding and ultimately controlling this phenomenon is an important issue in numerous biotechnologically-related fields, such as affinity-based separations, biomaterials science, and biosensor development.[3] Developing a fundamental understanding of protein adsorption behavior has consequently been a very active research area. Two recent reviews[1] discussed the major scientific issues currently being addressed by numerous research groups studying immobilized protein films, as well as progress and prospects. One of these issues, molecular orientation, is the major subject of this study and the accompanying paper.

Due to the inherently asymmetric distribution in physical/chemical properties and biofunctional sites on the surface of a protein, the geometric orientation of an adsorbed protein molecule may (i) differ among adsorbent surfaces having the different physical and chemical properties and (ii) determine if the molecule's native bioactivity is retained in the interfacial environment. For example, the orientation of an adsorbed protein may differ on hydrophilic and hydrophobic surfaces,[4] and may affect its ability to participate in electron transfer[5] or bind to a dissolved ligand.[6] Experimentally observed differences in surface activity and biofunction among protein-surface combinations have frequently been attributed to differences in molecular orientation.[5−12] Unfortunately, systematic investigation of these relationships has been limited by the experimental difficulty of measuring molecular orientation in a protein monolayer adsorbed at a solid−liquid interface.

Some progress has been made using polarized spectroscopic techniques such as resonance Raman scattering, total internal reflection fluorescence, and absorbance linear dichroism applied to protein films immobilized on a variety of different substrate materials.[4,13−19a] However, the individual application of any of these techniques cannot generate information on the distribu-

* To whom correspondence should be addressed. Phone: (520) 621-9761. Fax: (520) 621-8407. E-mail: sssaaved@ccit.arizona.edu.

[⊗] Abstract published in *Advance ACS Abstracts,* January 1, 1997.

(1) (a) Brash, J. L.; Horbett, T. A. In *Proteins at Interfaces II*, Horbett, T. A., Brash, J. L., Eds.; ACS Symposium Series 602; American Chemical Society: Washingotn, DC, 1995; pp 1−23 and references therein. (b) Hlady, V.; Buijs, J. *Curr. Opin. Biotechnol.* **1996**, *7*, 72−77 and references therein.

(2) (a) Andrade, J. D.; Hlady, V. *Adv. Polym. Sci.* **1986**, *79*, 1−63. (b) Haynes, C. A.; Norde, W. *Colloids Surf. B: Biointerfaces* **1994**, *2*, 517−566.

(3) Swalen, J. D.; Allara, D. L.; Andrade, J. D.; Chandross, E. A.; Garoff, S.; Israelchvili, J.; McCarthy, T. J.; Murray, R.; Pease, R. F.; Rabolt, J. F.; Wynne, K. J.; Yu, H. *Langmuir* **1987**, *3*, 932−950.

(4) Lee, J. E; Saavedra, S. S. *Langmuir* **1996**, *12*, 4025−4032.

(5) (a) Tarlov, M. J.; Bowden, E. F. *J. Am. Chem. Soc.* **1991**, *113*, 1847−1849. (b) Cullison, J. K.; Hawkridge, F. M.; Nakashima, N.; Yoshikawa, S. *Langmuir* **1994**, *10*, 877−882.

(6) (a) Chang, I.-N.; Herron, J. N. *Langmuir* **1995**, *11*, 2083−2089. (b) Lin, J.-N.; Chang, I.-N.; Andrade, J. D.; Herron, J. N.; Christensen, D. A. **1991** *J. Chromatogr. 542*, 41−54.

(7) (a) Spinke, J.; Liley, M.; Guder, H.-J.; Angermaier, L.; Knoll, W. *Langmuir* **1993**, *9*, 1821−1825. (b) Müller, W.; Ringsdorf, H.; Rump, E.; Wildburg, G.; Zhang, X.; Angermaier, L.; Knoll, W.; Liley, M.; Spinke, J. *Science* **1993**, *262*, 1706−1708.

(8) Hamachi, I.; Noda, S.; Kunitake, T. *J. Am. Chem. Soc.* **1991**, *113*, 9625−9630.

(9) Iuliano D. J.; Saavedra, S. S.; Truskey, G. A. *J. Biomed. Mater. Res.* **1993**, *27*, 1103−1113.

(10) Darst, S. A.; Robertson, C. R.; Berzofsky, J. A. *Biophys. J.* **1988**, *53*, 533−539.

(11) Lee, C.-S.; Belfort, G. *Proc. Natl. Acad. Sci. U.S.A.* **1989**, *86*, 8392−8396.

(12) Koyama, K.; Yamaguchi, N.; Miyasaka, T. *Science* **1994**, *265*, 762−765.

(13) Stayton, P. S.; Ollinger, J. M.; Jiang, M.; Bohn, P. W.; Sligar, S. G. *J. Am. Chem. Soc.* **1992**, *114*, 9298−9299.

(14) Hong, H.-G.; Bohn, P. W.; Sligar, S. G. *Anal. Chem.* **1993**, *65*, 1635−1638.

(15) Pachence, J. M.; Amador, S.; Maniara, G.; Vanderkooi, J.; Dutton, P. L.; Blasie, J. K. *Biophys. J.* **1990**, *58*, 379−389.

(16) Macdonald, I. D. G.; Smith, W. G. *Langmuir* **1996**,*12*, 706−713.

(17) (a) Walker, D. S.; Hellinga, H. W; Saavedra, S. S.; Reichert, W. M. *J. Phys. Chem.* **1993**, *97*, 10217−10222. (b) Lee, J. E; Saavedra, S. S. In *Proteins at Interfaces II*; Horbett, T. A., Brash, J. L., Eds.; ACS Symposium Series 602; American Chemical Society: Washington, DC, 1995; pp 269−279.

(18) Fraaije, J. G. E. M.; Kleijn, J. M.; van der Graaf, M.; Dijt, J. C. *Biophys. J.* **1990**, *57*, 965−975.

S0002-7863(96)02366-9 CCC: $14.00

tion of heme orientations in a protein film, since only one order parameter can be obtained by measuring a spectral parameter in only one dimension (e.g., intensity as a function of the excitation beam polarization in a fluorescence anisotropy experiment).

Information about the orientation distribution can be recovered by measuring at least two independent parameters.[20] Employing this general approach, several groups have determined dipole orientation distributions in molecular films adsorbed to silica glasses and indium tin oxide, and in Langmuir−Blodgett (LB) films doped with amphiphilic dyes.[21−24] With respect to protein films, the only study was reported by Bos and Klein.[22] Their attempt to determine the porphyrin orientation distribution in films of free base cytochrome *c* adsorbed on glass and indium tin oxide was unsuccessful due to scatter in the data.

In a previous paper,[24] we described a method for determining the dipole orientation distribution in a molecular film using a combination of two techniques: absorption linear dichroism, measured in a planar integrated optical waveguide-attenuated total reflection (IOW-ATR) geometry, and emission anisotropy, measured in a total internal reflection fluorescence (TIRF) geometry. The mean dipole tilt angle and angular distribution about the mean are recovered by using a Gaussian model for the dipole orientation probability. We successfully tested the IOW-ATR + TIRF method on model molecular assemblies consisting of LB films of arachidic acid doped with fluorescent amphiphiles.

Here we have extended this method to investigate molecular orientation in submonolayer to monolayer thick films of cytochrome *c* adsorbed to substrates of differing surface chemistry. Specifically, we examined if a macroscopically oriented protein film can be produced via "nonspecific" adsorption at a solid−liquid interface. The data presented below are the first reported orientation distribution measurements for protein film assemblies. The results show that an adsorbed cytochrome *c* (cyt *c*) film with a narrow orientation distribution can be produced when a single, high-affinity type of noncovalent binding occurs between the surface of the protein and the substrate surface. When multiple, competing adsorptive interactions are operative, a relatively disordered film will be produced. Although in retrospect these results are not surprising, their observation is unprecedented.

Theory

In a previous paper,[24] the IOW-ATR + TIRF method was used to determine the molecular orientation distribution in a thin film of linear dipole oscillators. In this study, a metalloporphyrin (heme) is used as a spectroscopic probe of macroscopic molecular order, which requires that some modifications to the theory used in the earlier paper be outlined.

The laboratory coordinate system is illustrated in Figure 1 using the geometry and notation of Thompson et al.[19b] and Fraaije et al.[18] Light propagating along the *x*-axis is totally internally reflected at the origin, which is at the interface (the $x-y$ plane) between the internal reflection element (IRE) and the adjacent medium of lower refractive index. The polarization of the evanescent field that decays exponentially along the positive *z*-axis from the origin is either transverse magnetic (TM) or transverse electric (TE). In TM polarization, the electric field projects primarily along the *z*-axis, with a small *x*-axis component, whereas in TE polarization, the electric field projects solely along the *y*-axis. A film of protein molecules, in which each molecule contains one heme, is located at the interface in the adjacent medium (although only one heme group is illustrated). The chromophores partially absorb the evanescent field and subsequently emit fluorescence.

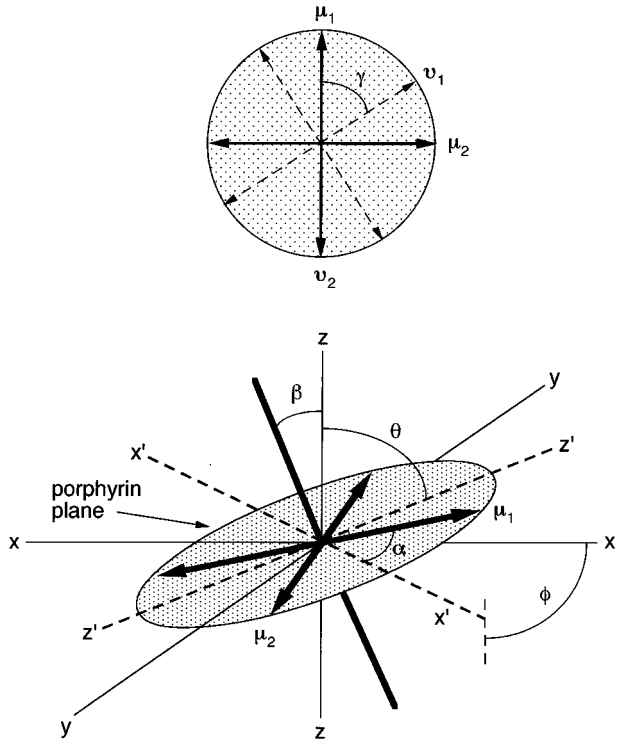

Figure 1. Top: Schematic of the molecular plane of a heme viewed along the normal axis. The absorption dipoles μ_1 and μ_2 are perpendicular to one another in the heme plane, as are the emission dipoles υ_1 and υ_2. The angle between μ_1 and υ_1 is γ. Bottom: Schematic of the heme molecular plane oriented in the laboratory coordinate system, defined by the *x*-, *y*-, and *z*-axes. The origin is at the point of reflection in the $x-y$ plane, which is the boundary between the total internal reflection element and the adjacent medium of lower refractive index. The heme is located at the interface in the lower index medium. The molecular plane, defined by the $x'-z'$ plane, lies at a polar angle θ from the *z*-axis. The angle between the *z*-axis and the normal to the molecular plane is β. The angle α describes the orientation of μ_1 in the $x'-z'$ plane, while ϕ is the azimuthal angle between the *x*- and x'-axes.

Ignoring the presence of side chains on the porphyrin ring, the heme exhibits D_{4h} symmetry due to the complexed metal ion. The two absorption transition dipoles, μ_1 and μ_2, are oriented perpendicular to each other in the heme plane, which is designated as the $x'-z'$ plane. The position of the heme plane relative to the laboratory coordinate system can be described by θ, which is the angle between the IRE surface normal (*z*-axis) and the heme plane, or β, the angle between the IRE surface normal and the normal to the heme plane. (Note that $\theta + \beta = 90°$.)

The in-plane orientation is described by the azimuthal angle, ϕ, the angle between the *x* and x' axes, and α, the angle between the μ_1 and the z' axis. Two emission transition dipoles, υ_1 and υ_2, are also oriented perpendicular to each other in the molecular plane. The angle between the absorption and emission dipoles, γ, is an expression of the extent of emission depolarization in

(19) (a) Timbs, M. M.; Thompson, N. L. *Biophys. J.* **1990**, *58*, 413−428. (b) Thompson, N. L.; McConnell, H. M.; Burghardt, T. P. *Biophys. J.* **1984**, *46*, 739−747.

(20) Szabo, A. *J. Chem. Phys.* **1980**, *72*, 4620−4626.

(21) (a) Wirth, M. J.; Burbage, J. D. *Anal. Chem.* **1991**, *63*, 1311−1317. (b) Burbage, J. D.; Wirth, M. J. *J. Phys. Chem.* **1992**, *96*, 5943−5948. (c) Wirth, M. J.; Piasecki-Coleman, D. A.; Montgomery, Jr., M. E. *Langmuir* **1995**, *11*, 990−995.

(22) (a) Bos, M. A.; Kleijn, J. M. *Biophys. J.* **1995**, *68*, 2573−2579. (b) Bos, M. A.; Kleijn, J. M. *Biophys. J.* **1995**, *68*, 2566−2572.

(23) LeGrange, J. D.; Riegler, H. E.; Zurawsky, W. P.; Scarlata, S. F. *J. Chem. Phys.* **1989**, *90*, 3838−3842.

(24) Edmiston, P. L.; Wood, L. L.; Lee, J. E.; Saavedra, S. S. *J. Phys. Chem.* **1996**,*100*, 775−784.

the plane of the heme. For a metalloporphyrin with D_{4h} symmetry, the emission should be nearly randomized in the molecular plane (i.e., circularly polarized with $\gamma = 45°$). However, the influence of the local environment around the heme, such as the presence of side chains and axial ligands, may cause γ to be less than 45°.

The steady state fluorescence anisotropy is defined as

$$r = \frac{I_z - I_y}{I_z + 2I_y} \tag{1}$$

where I_z and I_y are the emission intensities for excitation light polarized along the *z*-axis and *y*-axis excitation, respectively. Assuming that (i) absorption intensity is randomized in the heme plane (i.e., the magnitudes of μ_1 and μ_2 are equal),[25] (ii) the fluorescence is collected by a low numerical aperture objective so that emission intensity is proportional to the projection of v_i on the $x-y$ detection plane, (iii) the detection system exhibits zero polarization bias, (iv) no emission depolarization results from molecular motion or intermolecular energy transfer during the excited state lifetime, and (v) the angular distribution of adsorption and emission dipoles is isotropic with respect to ϕ and α (i.e., the distribution function $N(\phi) = 1$ and $N(\alpha) = 1$[24]), then the measured intensities can be related to molecular orientation by the following expressions:

$$I_z = E_z^2\langle(\sin^2\beta)(\sin^2\gamma + \cos^2\gamma\cos^2\beta)\rangle \tag{2}$$

$$I_y = (1/2)E_y^2\langle(1 + \cos^2\beta)(\cos^2\gamma + \sin^2\gamma\cos^2\beta)\rangle \tag{3}$$

In these equations E_y^2 and E_z^2 are the squared electric field amplitudes of the evanescent wave along the *y*- and *z*-axes at the origin and the angular brackets denote an ensemble average over all the heme groups in the film.

The measured anisotropy can be related to the angular distribution of polar tilt angles, $N(\beta)$, by integration of the β distribution functions, as expressed in eqs 4 and 5. Integration about β is necessary to extract information about the orientation distribution since the normal to the heme plane is the major symmetry axis of the molecule.

$$\frac{I_z}{E_z^2} = \frac{\int_0^{\pi/2} N(\beta)(\sin^2\beta)(\sin^2\gamma + \cos^2\gamma\cos^2\beta)\sin\beta\,d\beta}{\int_0^{\pi/2} N(\beta)\sin\beta\,d\beta} \tag{4}$$

$$\frac{I_y}{E_y^2} = \frac{1}{2}\frac{\int_0^{\pi/2} N(\beta)(1 + \cos^2\beta)(\cos^2\gamma + \sin^2\gamma\cos^2\beta)\sin\beta\,d\beta}{\int_0^{\pi/2} N(\beta)\sin\beta\,d\beta} \tag{5}$$

The functional form of $N(\beta)$ can be modeled as a Gaussian distribution,[21,24] where the heme planes are oriented about a mean tilt angle, β_μ, with an angular distribution (standard deviation) of β_σ:

$$N(\beta) = \exp\left[\frac{-(\beta - \beta_\mu)^2}{2\beta_\sigma^2}\right] \tag{6}$$

Since $N(\beta)$ is a function of two variables, a steady-state anisotropy measurement cannot be used alone to determine both β_μ and β_σ. This limitation is overcome by measuring absorption linear dichroism, in an IOW-ATR geometry, on protein film samples prepared under conditions identical to those used to prepare films for TIRF anisotropy measurements.

The basic theory for determining the mean porphyrin tilt angle in a heme protein film using IOW-ATR linear dichroism has been described previously.[4,17b] However, in previous studies, a δ function was used as an approximation of the orientation distribution in order to extract a mean tilt angle. This assumption is valid if the actual distribution is very narrow; however, if the actual distribution is broad (i.e., if $\beta_\sigma > 15°$ for the Gaussian model), then the calculated mean angle may differ substantially from the true mean angle. In this work, an integrated form of the expression that relates β to the measured linear dichroic ratio (ρ) is used in place of the equation employed in earlier studies (i.e., eq 3 in ref 4). This substitution eliminates the need to assume that the distribution function is very narrow. The expression is

$$\rho = \frac{A_{f,TE}}{A_{f,TM}}\left(\frac{N_{TM}}{N_{TE}}\right) = \frac{(1/2)E_y^2\int_0^{\pi/2} N(\beta)(1 + \cos^2\beta)\sin\beta\,d\beta}{(1/2)E_x^2\int_0^{\pi/2} N(\beta)(1 + \cos^2\beta)\sin\beta\,d\beta + E_z^2\int_0^{\pi/2} N(\beta)\sin^2\beta\sin\beta\,d\beta} \tag{7}$$

where $N(\beta)$ is the orientation distribution function (assumed to be Gaussian), $A_{f,TE}$ and $A_{f,TM}$ are the absorbance values due to the film for light propagating in the pair of TE and TM polarized modes under comparison, N is the number of total internal reflections over which the measurement is made in each mode, and E_x^2, E_y^2, and E_z^2 are the squared electric field amplitudes of the evanescent wave along the *x*-, *y*-, and *z*-axes at the origin. Expressions for calculating N and the electric field amplitudes, using the ray optics and two-phase approximations,[26,27] are given in refs 17b and 26.

Measuring two parameters, r and ρ, allows values for β_μ and β_σ to be calculated simultaneously using eqs 1−7. To maintain consistency with previous work,[4,17,24] orientation distributions reported in this paper are stated in terms of θ rather than β.

Experimental Section

Zinc 5,10,15,20-Tetrakis(4-octadecylpyridinio)porphyrin (Zn-TOPP). TOPP was synthesized from 5,10,15,20-tetrakis-4-pyridyl-21*H*,23*H*-porphine (Aldrich, 97%) and 1-bromooctadecane (Aldrich, 96%), using the procedure described by Ruaudel-Teixier et al.[28a] The visible absorbance spectrum of TOPP (methanol solution) had bands centered at 422, 518, 552, 592, and 648 nm, which corresponds closely to the spectral features of 5,10,15,20-tetrakis(3-eicosylpyridinio)-porphyrin bromide, a very similar compound.[28a] The infrared spectral features also corresponded. Zn-TOPP was prepared from TOPP and $ZnCl_2$, following well-known procedures.[28b] The visible absorption spectrum of Zn-TOPP dissolved in chloroform exhibited bands centered at 442, 525, 574, and 616 nm. Zinc 5,10,15,20-tetra-4-pyridylporphyrin was prepared in a similar manner.

Silanes. Undecylenyl acetate was prepared by combining ω-undecylenyl alcohol (3.5 mL, 0.0187 mol) with triethylamine (3.9 mL, 0.0187 mol) and cooling the stirred mixture to 0 °C under nitrogen. To this solution was added, dropwise with stirring over a 30 min period, a mixture of acetyl chloride (1.23 mL, 0.0224 mol) and 50 mL of dichloromethane. The mixture was stirred for an additional 1.5−2 h, then washed sequentially with cold water, 5% HCl, 20% $NaHCO_3$, and

(25) Hofrichter, J.; Eaton, W. A. *Annu. Rev. Biophys. Bioeng.* **1976**, 5, 511−560.

(26) Saavedra, S. S.; Reichert, W. M. *Anal. Chem.* **1990**, *62*, 2251−2256.

(27) Reichert, W. M. *Crit. Rev. Biocompat.* **1989**, *5*, 173−205.

(28) (a) Ruaudel-Teixier, A.; Barraud, A.; Belbeoch, B.; Roulliay, M. *Thin Solid Films* **1983**, *99*, 33−40. (b) Dorough, G. D.; Miller, J. R.; Huennekens, F. M. *J. Am. Chem. Soc.* **1951**, 73, 4315−4320.

saturated aqueous NaCl, dried with $MgSO_4$, filtered, and concentrated by rotary evaporation. Purification was done by flash chromatography using 5% ethyl acetate−hexane as the eluent. The product, undecylenyl acetate, was then used to prepare 1-acetato-11-(trichlorosilyl)undecane following the procedure reported in ref 29. 1-(Thioacetato)-16-(trichlorosilyl)hexadecane was prepared according to the procedure described in ref 29.

Protein Solutions. Ferricytochrome *c* from horse heart (ferricyt *c*; Sigma, 99%) was dissolved in 50 mM phosphate buffer, pH 7.2, purified by gel filtration on Sephadex G-25, and further diluted with phosphate buffer to the final concentration required in particular experiments (using $\epsilon_{410\ nm} = 106\ 100\ M^{-1}\ cm^{-1}$ [30]). Ferrocyt *c* was prepared using a molar excess of sodium dithionite. After purification on a Sephadex G-25 column, ferrocyt *c* solution was saturated with argon gas to prevent reoxidation, and used immediately after dilution to the final concentration required in particular experiments (using $\epsilon_{416\ nm} = 129\ 100\ M^{-1}\ cm^{-1}$ [30]). Porphyrin cyt *c* was prepared following published procedures.[31] Zinc-substituted cyt *c* (Zn-cyt *c*) was prepared as described by Vanderkooi et al.[31b] The product was dialyzed against 50 mM ammonium acetate, pH 5.0, for 6 h and then overnight against 50 mM phosphate buffer, pH 7.2. Zn-cyt *c* concentration was determined using $\epsilon_{423\ nm} = 243\ 000\ M^{-1}\ cm^{-1}$ [32]).

Bovine serum albumin (BSA; fraction V, Sigma) derivatized with fluorescein isothiocyanate (FITC; Molecular Probes) was prepared following the vendor's instructions.[32] Using absorbance spectrometry, a fluorescein:BSA molar ratio of 0.7 was determined for the product.

Substrate Cleaning and Silane Deposition. Silicon oxynitride planar waveguides[33] and sol−gel glass planar waveguides[34] were used as substrates for linear dichroism experiments. Fused silica slides (2.5 cm × 7.5 cm × 1 mm thick, Dynasil, Berlin, NJ) were used as substrates for TIRF anisotropy experiments. Clean, hydrophilic substrates and substrates coated with dichlorodimethylsilane (DDS) were prepared as described previously.[4] Substrates were either used immediately or stored in a sealed container at room temperature in the dark until use. The surfactant 1-(thioacetato)-16-(trichlorosilyl)-hexadecane was used to prepare substrates coated with self-assembled monolayers (SAMs) bearing a thiol tail group. Hydrophilic substrates were immersed into a 0.1% (3−4 mM) solution of the surfactant dissolved in dicyclohexyl (Aldrich) for 4−5 h. The substrates were then copiously washed with chloroform, acetone, and deionized water, dried under a stream of nitrogen, and stored in a sealed container at room temperature in the dark until use. Just prior to use, the thioacetate tail group was reduced to a thiol by immersing the substrate into a solution of ether saturated with $LiAlH_4$ for about 30 s. The substrate was then washed sequentially in 4% HCl, chloroform, acetone, and deionized water and dried under a stream of nitrogen. The reduction process was repeated two times to ensure complete conversion of the thioacetate to the thiol, producing a SAM composed of covalently bound $C_{16}SH$ moieties. Using 1-acetato-11-(trichlorosilyl)undecane, substrates coated with $C_{11}OH$ SAMs were prepared in an identical manner. These coatings are referred to below as thiol and hydroxy SAMs, respectively. Static water contact angles[4] for hydrophilic, DDS-coated, thiol SAM-coated, and hydroxy SAM-coated substrates were 10° ± 6°, 88° ± 1°, 72° ± 2°, and 45° ± 2°, respectively.

Langmuir−Blodgett (LB) Film Deposition. LB films containing Zn-TOPP consisted of five layers: three layers of pure cadmium arachidate (CdA) followed by two layers of arachidic acid (AA) doped with Zn-TOPP. The deposition procedure was essentially identical to that described previously.[24] The Zn-TOPP:AA molar ratio in the spreading solution was 1:150. Transfer ratios were near unity except for the second CdA layer, which was typically 0.85. On planar waveguide substrates, the Zn-TOPP/AA layers were deposited over only half of the total CdA film area. The other half was not coated to enable the blank propagation loss of the CdA-coated waveguide structure to be measured, as described previously.[24] Spectroscopic measurements on Zn-TOPP films were performed within 24 h of deposition.

For protein adsorption studies, LB multilayer films containing pure AA in the outer layer, in a "headgroup-out" orientation, were prepared in a similar manner. Three layers of CdA were first deposited, followed by a single AA layer. The substrate was then released from the dipping mechanism into a Teflon container that had been placed in the subphase prior to film deposition. This allowed the film to remain under water during subsequent manipulations, which prevented the headgroup-out surface from being exposed to air.

IOW-ATR Linear Dichroism Measurements. Absorption linear dichroism on waveguide-supported LB films doped with Zn-TOPP was measured at 457.9 nm, using the instrumental arrangement and procedures described in ref 24. Measurements on protein films were performed at 514.5 nm, following the experimental protocols described in ref 4.

Dichroic ratios measured on identically prepared samples coated on different waveguides were used to compute mean values and respective standard deviations. Since the mode propagation angle differed among waveguides, individual ρ measurements were first normalized to the mode-dependent parameters (number of total internal reflections and the squared electric field amplitudes of the evanescent wave). In the case of TM polarized light, a correction was also made for the non-zero E_x^2 component present in the denominator of eq 7. All ρ values reported below were corrected using this procedure, which is described in the Supporting Information for this paper. After the correction procedure is applied, eq 7 can rewritten as

$$\rho = \frac{A_{f,TE,corrected}}{A_{f,TM,corrected}} = \frac{(1/2)\int_0^{\pi/2} N(\beta)(1+\cos^2\beta)\sin\beta\, d\beta}{\int_0^{\pi/2} N(\beta)\sin^2\beta\sin\beta\, d\beta} \quad (8)$$

Intrinsic Anisotropy Measurements. The intrinsic anisotropy (r_o) of Zn-cyt *c* was measured using a solution containing 3 μM protein in 97:3 (v/v) glycerol/phosphate buffer (50 mM, pH 7). The measurements were performed at excitation and emission wavelengths of 582 and 636 nm, respectively. The mean angle (γ) between the absorption and emission dipoles was calculated from[36]

$$r_o = \frac{I_v - I_h}{I_v + 2I_h} = \frac{2}{5}\left[\frac{3\cos^2\gamma - 1}{2}\right] \quad (9)$$

where I_v and I_h are the fluorescence intensities measured with the emission polarizer oriented parallel and perpendicular, respectively, to the vertically oriented excitation polarizer. For zinc 5,10,15,20-tetra-4-pyridylporphyrin, r_o was determined in an identical manner.

TIRF Measurements. TIRF anisotropy measurements on Zn-TOPP-doped LB films were performed using modifications of the instrumental arrangement and procedures described previously.[24] The 575 nm output from a Coherent 599 dye laser was used for excitation. The collected fluorescence was directed through a bandpass filter (635DF35, Omega Optical) onto a liquid nitrogen cooled CCD camera (Photometrics). Since Zn-TOPP fluorescence should be nearly circularly polarized,[37] no emission polarizer was present in the detection path. The size of the image of the TIRF excitation spot on the CCD chip was typically 100 × 200 pixels. Intensity measurements were made by summing the pixel intensities over this area, using 5 × 5 binning and integrating for 1−5 s. The total number of pixel counts was typically 10^6−10^7. The mean background intensity was obtained by imaging the sample without laser illumination at each spot on the film where polarization was measured.

For experiments with protein films, the slide was fitted to a liquid cell fabricated from Plexiglas (Figure 2). Experiments were initiated by exchanging the water in the cell for about 3−5 mL of protein

(29) Balachander, N.; Sukenik, C. N. *Langmuir* **1990**, *6*, 1621−1627.
(30) Margoliash, E.; Frohwirt, N. *Biochem. J.* **1959**, *71*, 570−572.
(31) (a) Robinson, A. B.; Kamen, M. D. In *Structure and Function of Cytochromes*; Okunuki, K., Kamen, M. D., Sekuzu, I., Eds.; University Park Press: Baltimore, 1968; pp 383−387. (b) Vanderkooi, J. M.; Adar, F.; Erecinska, M. *Eur. J. Biochem.* **1976**, *64*, 381−387.
(32) Conjugation With Amine Reactive Probes. technical bulletin; available from Molecular Probes, Eugene, OR.
(33) Walker, D. S.; Reichert, W. M.; Berry, C. J. *Appl. Spectrosc.* **1992**, *46*, 1437−1441.
(34) Yang, L.; Saavedra, S. S.; Armstrong, N. R.; Hayes, J. *Anal. Chem.* **1994**, *66*, 1254−1263.
(35) Yang, L.; Saavedra, S. S. *Anal. Chem.* **1995**, *67*, 1307−1314.
(36) Lakowicz, J. R. *Principles of Fluorescence Spectroscopy*, Plenum: New York, 1983; p 120.
(37) Gouterman, M.; Stryer, L. *J. Chem. Phys.* **1962**, *37*, 2260−2266.

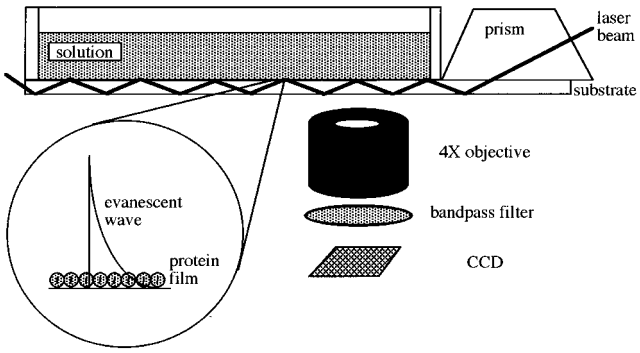

Figure 2. Diagram of the flow cell for TIRF anisotropy measurements. The drawing is not to scale.

solution, which covered approximately 4 cm^2 of the surface of the slide. The protein solution was incubated in the cell for approximately 30 min in a humidified container under an argon atmosphere at room temperature. The solution was then replaced with phosphate buffer, without allowing the protein-coated surface of the slide to be exposed to air. Anisotropy measurements on cyt *c* films were performed in a manner identical to that employed for LB films containing Zn-TOPP. This was also true for FITC−BSA films, except that, in place of the 615 nm bandpass filter, a sheet polarizer and a 515 nm bandpass filter (515EFLP, Omega Optical) were placed between the microscope objective and the CCD. In all cases, the raw emission intensity measurements in TE and TM polarizations, I_{TE} and I_{TM}, were corrected for polarization-dependent differences in laser power and the nonzero E_x^2 component of TM excitation, using the procedures outlined previously,[24] to calculate the respective I_y and I_z values used in eq 1.

Orientation Distribution Calculations. For experiments on heme protein films and LB films containing Zn-TOPP, the mean tilt angle (β_μ) and the angular distribution (β_σ) were recovered by iteratively substituting estimated values for β_μ and β_σ into eqs 1 and 8, such that the calculated anisotropy (r) and dichroic ratio (ρ) matched the measured mean values for r and ρ as closely as possible. Integrations were performed using Mathematica software (Wolfram Research). For consistency with previous work,[4,17,24] β_μ and β_σ values were converted to and reported as θ_μ and θ_σ, respectively. The equations and method for determining θ_μ and θ_σ for films containing FITC (a linear dipole) were described in an earlier paper.[24]

Protein Surface Coverages. A surfactant desorption assay was used to measure the surface coverages of cyt *c* adsorbed to hydrophilic and silane-coated surfaces. Glass beads (3 mm diameter, Baxter) were used as substrates to increase the surface area relative to planar substrates. Hydrophilic beads and beads derivatized with the DDS, $C_{11}OH$, and $C_{16}SH$ coatings were prepared using the procedures described above for planar substrates, except the deposition time was increased to 6−7 h and, for $C_{11}OH$ and $C_{16}SH$, the silane concentrations were increased to 0.3%. Ferricyt *c* was incubated with approximately 20 g of beads in a clean glass vial for 30 min to effect adsorption (under conditions equivalent to those used for planar substrates) and then rinsed with phosphate buffer. The adsorbed protein was then desorbed and the surface coverage determined as described previously.[4]

Planar substrates (2.5 cm × 7.5 cm × 1 mm glass slides) were used for surface coverage determinations of cyt *c* adsorbed to LB films. Eight headgroup-out LB films were incubated for 45 min in a solution containing a 2:3 molar ratio of Zn-cyt *c*/ferricyt *c*, with a total protein concentration of 50 μM. The ratio of substrate surface area to volume of protein solution was approximately the same as used in the linear dichroism and fluorescence anisotropy experiments. After washing with phosphate buffer, the slides were immersed in a Teflon cell containing 10 mL of 1% (v/v) Triton X-100 in 200 mM KCl and sonicated for 10 min. Essentially quantitative desorption of protein was confirmed by epifluorescence microscopy. The concentration of desorbed cyt *c* in the sonicated solution was determined by fluorescence spectrometry, using a dilution series of Zn-cyt *c* dissolved directly in 1% Triton X-100/200 mM KCl to generate an external calibration curve. Surface coverages were calculated by ratioing the amount of desorbed protein to the aggregate surface area of the slides, under the applicable assumptions stated in ref 4.

Results and Discussion

We previously reported the development of a methodology, based on a combination of IOW-ATR linear dichroism and TIRF anisotropy measurements, to measure the orientation distribution of fluorescent dipoles in a substrate-supported, submonolayer film.[24] In that initial phase, we tested the IOW-ATR + TIRF method on model molecular assemblies consisting of Langmuir−Blodgett films of arachidic acid (AA) doped with linear dipole oscillators.

The primary goals of the present work were the following: (1) To extend molecular orientation distribution measurements, using the IOW-ATR + TIRF method, to thin film assemblies of heme proteins. A model molecular assembly, consisting of a LB multilayer of AA doped with Zn-TOPP, was used to test application of the method to a submonolayer film of circularly polarized oscillators, prior to proceeding to protein film samples. (2) To investigate the effect of substrate surface chemistry on molecular orientation in adsorbed monolayers of heme proteins. Orientation distributions were measured for a model heme protein, horse heart cyt *c*, adsorbed to several different surfaces: hydrophilic (bare) glass substrates, substrates derivatized with DDS, substrates coated with thiol and hydroxy SAMs, and substrates coated with Langmuir−Blodgett films of AA.

Theoretical Considerations. For the geometry illustrated in Figure 1, the theoretically allowable ranges for anisotropy and the dichroic ratio are −0.5 to +0.25 and 0 to infinity, respectively. As discussed previously,[24] it is important to note that the parameter space in which combinations of r and ρ are physically reasonable is considerably smaller. The relationship is illustrated in Figure 3, in which possible values for r, ρ, the mean tilt angle (θ_μ), and the angular distribution (θ_σ) for a circular dipole oscillator are plotted over the ranges of $-0.5 \leq r \leq +0.25$, $0 \leq \rho \leq 4$, $0° \leq \theta_\mu \leq 90°$, and $\pm 0° \leq \theta_\sigma \leq \pm 90°$. The response surfaces define those combinations of the parameters that are theoretically possible for a Gaussian orientation distribution model. It is evident that most of the parameter space represents combinations of r and ρ that are physically inconsistent. For example, a molecular assembly cannot have an anisotropy of 0.15 and a dichroic ratio of 4, which would correspond to heme plane orientations predominately perpendicular and parallel to the $x-y$ plane, respectively. This illustrates the "cross-checking" feature of the IOW-ATR + TIRF technique, which aids in detecting systematic errors. In other words, an angular distribution cannot be calculated if a given pair of measurements (r and ρ) are physically inconsistent.

Figure 3 also shows that r and ρ are more sensitive to the angular distribution when θ_μ is near 0° or 90°, and is relatively insensitive when θ_μ is near 35°. The trend is shown more clearly in Figure 4, in which anisotropy is plotted as a function of θ_σ over the range of ±5° to ±86° for four discrete values of θ_μ (5°, 35°, 60°, and 85°). When $\theta_\mu = 35°$, r can vary only from −0.056 to −0.089, which is an 11-fold smaller interval than when $\theta_\mu = 85°$, where r can vary from −0.475 to −0.105. Thus, a less precise evaluation of the width of the distribution can be obtained when $\theta_\mu = 35°$. (Note also that for a completely random orientation distribution, $\beta_\mu = 54.7°$ which means that $\theta_\mu = 35.3°$.)

LB Films Doped with Zn-TOPP. Studies of multilayer LB films prepared from pure pyridinioporphyrin derivatives, using resonance Raman and electron spin resonance spectroscopies, have shown that the porphyrin plane is aligned nearly parallel

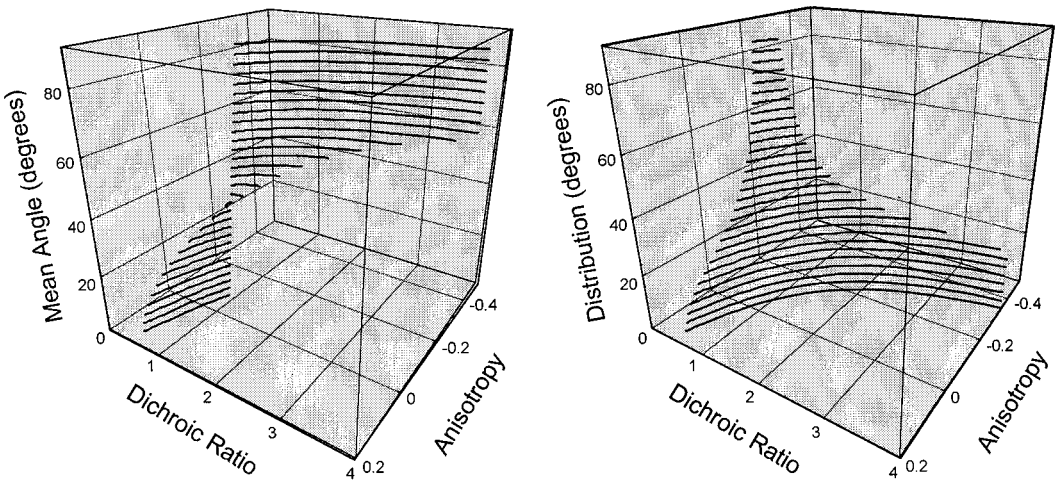

Figure 3. Response surfaces for a circularly polarized oscillator showing theoretically possible values of the mean tilt angle (A, top) and angular distribution (B, bottom). Calculations were performed using eqs 1 and 8 at a 3° interval for both θ_μ and θ_σ, for anisotropy values ranging from −0.5 to +0.2, for dichroic ratios ranging from 0 to 4, and assuming a value of 41° for γ.

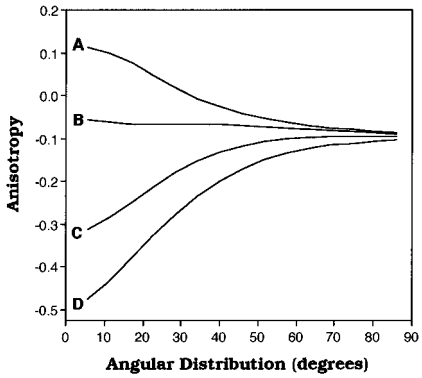

Figure 4. Relationship between anisotropy and angular distribution for several discrete mean tilt angles, assuming a value of 38° for γ: (A) $\theta_\mu = 5°$; (B) $\theta_\mu = 35°$; (C) $\theta_\mu = 60°$; (D) $\theta_\mu = 85°$.

to the film plane.[38] An LB bilayer film of arachidic acid doped with Zn-TOPP therefore appeared to be an appropriate assembly for testing the theoretical and instrumental approaches used in this study. It also served as a good model for comparison to results obtained for heme protein films. Experiments were performed on films of low surface coverage (about 1%) to prevent energy transfer between chromophores, which would invalidate the fluorescence anisotropy results (see the discussion below regarding Zn-cyt *c* films).

The macroscopic uniformity of films doped with Zn-TOPP was qualitatively analyzed by epifluorescence microscopy. The goal was to generate films that were devoid of observable structural features. Under 400× magnification, the fluorescence emission intensity from these films was macroscopically uniform. The characterization of undoped CdA/AA LB films by infrared spectroscopy, ellipsometry, and waveguide propagation loss measurements is described in a previous paper.[24]

Two planar waveguides coated with Zn-TOPP-doped films were prepared, and IOW-ATR linear dichroism measurements were performed at three distinct physical locations on each. The dichroic ratio (ρ) was 105 ± 42. (Note that the standard deviation of the measurement is large because $A_{f,TM}$, the denominator in eq 8, was very small, and the standard deviation does not provide any information about the distribution of tilt angles in the film.) TIRF measurements made on Zn-TOPP-doped films supported on fused silica substrates, prepared under otherwise identical conditions, yielded an anisotropy of −0.482 ± 0.009. The fact that $\rho > 10$ and r is very close to the theoretical minimum of −0.5 indicates that the molecular plane of Zn-TOPP is nearly parallel to the LB film plane (see Figure 3a).

Table 1. Orientation Distributions (deg) Calculated for Selected Combinations of Emission Anisotropy and Dichroic Ratio: Application to LB Films Doped with Zn-TOPP[a]

	anisotropy (r)		
dichroic ratio (ρ)	−0.473	−0.482 ± 0.009[b]	−0.491
63	n/o[c]	90 ± 5.7	89 ± 4.7
105 ± 42[b]	n/o	n/o	89 ± 3.6
147	n/o	n/o	87 ± 2.3

[a] Gaussian orientation distributions expressed as $\theta_\mu \pm \theta_\sigma$. [b] Measured ρ and r values (mean ± standard deviation) for AA LB films doped with Zn-TOPP. [c] Not obtainable (the combination of ρ and r did not produce a simultaneous solution to eqs 1 and 8).

However, substituting the mean values for ρ and r, and a value of 41° for γ (based on the intrinsic anisotropy measurements described below), into eqs 1 and 8 did not yield a calculated solution. In other words, the combination of $\rho = 105$ and $r = -0.482$ is physically inconsistent with a Gaussian distribution model for a circularly polarized oscillator with $\gamma = 41°$. However, orientation distributions could be calculated for other pairs of ρ and r that lie within 1 standard deviation of the mean values, as shown in Table 1. Within the ranges of $\rho = 105 \pm 42$ and $r = -0.482 \pm 0.009$, the calculated values for θ_μ and θ_σ fell in the ranges of 87−90° and ±2.3° to ±5.7°, respectively.

As the data in Table 1 make clear, the inability to calculate a distribution for the combination of $\rho = 105$ and $r = -0.482$ is a consequence of the very narrow range of allowable values that these parameters can assume when the porphyrin plane is tilted nearly 90°. With reference to Figure 3, it is apparent that an ensemble of circularly polarized oscillators must be distributed narrowly about a tilt angle of ca. 90° when r approaches −0.5 and ρ approaches positive infinity. Thus, the inability to calculate a distribution for $\rho = 105$ and $r = -0.482$ *cannot* be attributed to a systematic error in the experimental and theoretical approach. Rather this combination of measurements can only be interpreted as evidence of a highly ordered film, which is consistent with previous studies of molecular orientation in porphyrin-containing LB films.[38]

(38) (a) Lesieur, P.; Vandevyver, M.; Ruaudel-Teixier, A.; Barraud, A. *Thin Solid Films* **1988**, *159*, 315−322. (b) Palacin, S.; Ruaudel-Teixier, A.; Barraud, A. *J. Phys. Chem.* **1986**, *90*, 6237−6242.

In summary, over length scales on the order of 1 cm, (i) the angular distribution of porphyrin planes in Zn-TOPP-doped LB films is centered at a mean tilt angle nearly parallel to the film plane and (ii) the porphyrin planes are distributed in a very narrow range about the mean angle. Finally, the Zn-TOPP results demonstrate extension of the IOW-ATR + TIRF method to orientation distribution measurements on films containing circularly polarized oscillators.

Experimental Considerations for Fluorescence Measurements on Cyt *c* Films. In native cyt *c*, the fluorescence emission of the heme is quenched by the central iron atom. Therefore, to perform fluorescence anisotropy measurements, the protein had to be modified by removing the iron,[31] which produces free base cyt *c* in which the porphyrin exists as two tautomers with exchangeable hydrogens bound to two of the four central nitrogens.[18] The heme absorption dipoles are no longer degenerate,[18] which makes the theoretical analysis somewhat more complicated. Inserting a Zn atom into the porphyrin restores the approximately D_{4h} symmetry of the chromophore,[37] and was the approach employed here. The major disadvantage is that Zn-cyt *c* has a lower fluorescence quantum efficiency than free base cyt *c*.[32]

NMR studies of Zn-cyt *c* indicate that its conformation is not significantly perturbed relative to native cyt *c*.[39] However, removing the iron atom does alter the structural stability of the protein, possibly due to the absence of histidine−Fe ligation. This was confirmed by comparing the effect of a denaturing agent, guanidine HCl, on the intrinsic spectral properties of native ferricyt *c* and Zn-cyt *c*. The Soret band absorbance maximum and the tryptophan fluorescence intensity (which is quenched in the folded state because of energy transfer to the heme) of both proteins were monitored as a function of guanidine·HCl concentration. The denaturation midpoint of Zn-cyt *c* occured at a guanidine·HCl concentration of approximately 1.75 M while that of native ferricyt *c* was about 3 M. Despite this difference in structural stability, we assume that the surface activities of Zn-cyt *c* and native cyt *c* are equivalent with respect to all of the substrates examined in this study. Invoking this assumption permits Zn-cyt *c* to be used as a substitute for native cyt *c*, which in turn makes it possible for us to measure molecular orientation distributions in cyt *c* films using the IOW-ATR + TIRF method.

The mean angle (γ) between the absorption and emission dipoles of Zn-cyt *c* was determined by measuring the intrinsic emission anisotropy (r_o) of the protein dissolved in a viscous solvent at excitation and emission wavelengths of 582 and 636 nm, respectively**.** Using eq 9, a value of 41° was calculated for γ (mean of two measurements). For comparison, a γ value of 41° was also measured for zinc 5,10,15,20-tetra-4-pyridylporphyrin. Measurements of γ were not performed for adsorbed Zn-cyt *c*. For the purposes of this study, a constant value of 41° was assumed, regardless of whether the protein was dissolved or adsorbed at a solid−liquid interface.

Since nonradiative energy transfer between fluorophores in a close-packed molecular assembly results in depolarized emission, it must be eliminated if anisotropy measurements are to be used to quantitatively assess dipole orientation. In this study, TIRF anisotropy measurements were performed on adsorbed protein films formed by incubating substrates with solutions containing a 1:10 molar ratio of Zn-cyt *c*/ferrocyt *c*. Absorbance spectra of both proteins are plotted in Figure 5. Assuming a statistical distribution of molecules in a close-packed, randomly oriented protein monolayer, the average center-to-center distance between zinc porphyrin groups would be about 57 Å. This separation is large enough to theoretically eliminate almost all energy transfer between zinc porphyrins. Ferrocyt *c* was used as the diluent since the α/β absorbance bands of the heme are blue shifted relative to ferricyt *c* and therefore do not overlap the Zn-cyt *c* excitation band centered near 580 nm. This prevented energy transfer from Zn-cyt *c* to native cyt *c*, which would result in quenching and possibly eventual transfer to another Zn-cyt *c* molecule in the film. To test if a 1:10 molar ratio of Zn-cyt *c*/ferrocyt *c* was sufficient to prevent energy transfer in an adsorbed protein film, hydrophilic glass substrates were incubated with solutions containing 1:10, 1:20, and 1:30 molar ratios of Zn-cyt/ferrocyt *c*, with the total protein concentration held constant at 35 μM. The fluorescence anisotropy measurements performed on the resulting protein films were statistically equivalent, which supports the assumption that a 1:10 molar ratio is sufficiently dilute to prevent energy transfer in a Zn-cyt/ferrocyt *c* film.

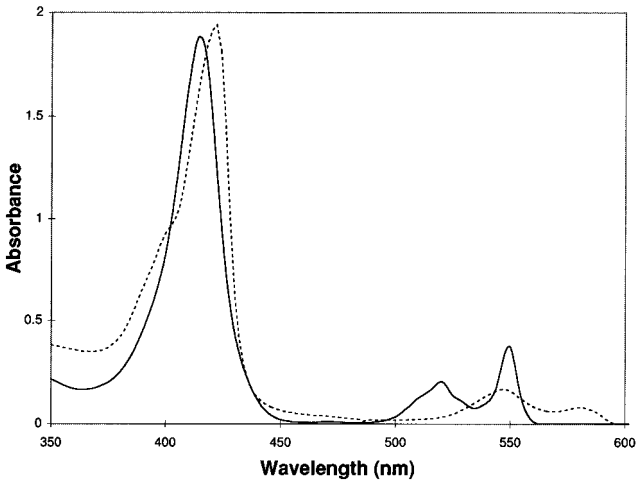

Figure 5. Absorbance spectra of 8 μM Zn-cyt *c* (dashed line) and 14 μM ferrocyt *c* (solid line) dissolved in 50 mM phosphate buffer, pH 7.2, in a 1 cm path length cuvette.

We conclude this section by stating a general assumption that must be invoked to enable the use of TIRF anisotropy measurements to examine molecular orientation in protein films containing Zn-cyt *c*: The molecular orientation distribution of Zn-cyt *c* molecules, coadsorbed in a film composed predominately of native cyt *c*, is equivalent to the molecular orientation distribution of all the protein molecules in the film. Although this assumption appears reasonable, we have not verified it independently.

Protein Surface Coverages. A surfactant desorption assay was used to determine protein surface coverages. The measurements were performed using the solution concentrations and incubation times listed for each substrate in Table 2. From the crystallographic dimensions of cyt *c* (25 × 25 × 37 Å),[40] a surface coverage of 2.2×10^{-11} mol/cm^2 is the equivalent of one monolayer, assuming that the orientation of the molecules in the film is geometrically random and no "spreading" occurs due to adsorption-induced conformational changes. The surface coverages listed in Table 2 are given in monolayer units and range from 0.4 on the hydroxy SAM to 1.4 on the arachidic acid LB film.

These measurements should be considered approximate. The standard deviations range up to 25%. A potentially greater source of uncertainty is the assumptions involved. As noted

(39) Moore, G. R.; Pettigrew, G. W. *Cytochromes c. Evolutionary, Structural, and Physicochemical Aspects*; Springer-Verlag: Berlin, 1990; p 24.

(40) Lvov, Y.; Ariga, K.; Ichinose, I.; Kunitake, T. *J. Am. Chem. Soc.* **1995**, *117*, 6117−6123.

Table 2. Surface Coverages and Orientation Distributions for Adsorbed Cytochrome *c* Films

substrate surface	bulk protein concentration[a] (μM)	adsorption time[a]	surface coverage (monolayers)[b]	dichroic ratio (ρ)	anisotropy (r)	orientation distribution ($\theta_\mu \pm \theta_\sigma$, deg)
hydrophilic glass	35	30 min	1.3 ± 0.29 ($n = 3$)	0.59 ± 0.05 ($n = 2$)	-0.021 ± 0.019 ($n = 3$)	12 ± 33[d]
thiol SAM-coated glass	35	3 h	0.5	1.66 ± 0.23 ($n = 3$)	-0.176 ± 0.030 ($n = 5$)	61 ± 23[d]
hydroxy SAM-coated glass	35	8−10 h	0.4	0.70 ± 0.03 ($n = 3$)	-0.053 ± 0.023 ($n = 3$)	13 ± 29
DDS-treated glass	35	30 min	0.8 ± 0.21 ($n = 3$)	1.58 ± 0.03 ($n = 3$)	-0.188 ± 0.013 ($n = 6$)	49 ± 11
arachidic acid LB film	50	30 min	1.4	1.54 ± 0.17 ($n = 7$)	-0.154 ± 0.026 ($n = 3$)	46 ± 6

[a] Concentration of protein solution and amount of time that solution was incubated with substrate to effect adsorption. [b] Based on one monolayer $= 2.2 \times 10^{-11}$ mol/cm^2. Unless otherwise noted, $n = 1$ for all measurements. [c] Distribution is representative of the range of distributions listed in Table 3. [d] Distribution is representative of the range of distributions listed in Table 4.

above, the mean surface area occupied by an adsorbed protein molecule is not known (and may differ among the various surface chemistries). Furthermore, to correlate molecular orientation and surface coverage measurements on protein films adsorbed to different materials (e.g., fused silica slides and soda lime glass beads), one must assume that the adsorption behavior on the two glass types is similar and that the surface roughness of the two materials is also similar. Despite the uncertainties, the results are consistent with known trends. At pH 7, the net charge on cyt *c* is +9 and distributed asymmetrically,[41] which presumably is the cause of its well-known tendency to adsorb strongly to negatively charged surfaces, such as membranes containing anionic lipids or fatty acids.[42] On the basis of its neutral, hydrophilic character, the surface of the hydroxy SAM would be expected to exhibit the lowest affinity for protein adsorption,[1,2] which is consistent with our observations.

Orientation Distributions in Adsorbed Cyt *c* Films. IOW-ATR linear dichroism and TIRF anisotropy measurements were performed on adsorbed cyt *c* films prepared using the solution concentrations and incubation times listed for each substrate in Table 2. The results of these experiments (dichroic ratio, anisotropy, and calculated orientation distribution, expressed as $\theta_\mu \pm \theta_\sigma$) are also listed in Table 2.

For two of the substrates, hydrophilic glass and thiol SAM-coated glass, orientation distributions could not be calculated from the respective pairs of measured mean values for ρ and r. In other words, the mean values were physically inconsistent with a Gaussian distribution model for a circularly polarized oscillator with $\gamma = 41°$. The cause(s) of this inconsistency are unknown, but the most likely is random measurement error (as discussed above for the Zn-TOPP-doped LB films). Other possibilities include (i) γ may not be 41° if the native protein structure is perturbed in the interfacial environment and (ii) a Gaussian model may be inappropriate for this sample.

However, in the case of cyt *c* adsorbed to hydrophilic glass, orientation distributions could be calculated for other pairs of ρ and r that were close to the respective mean values of 0.59 and −0.021. (This suggests that random measurement error is the primary cause of the physical inconsistency.) The results of the calculations are shown in Table 3. All of the orientation distributions listed there have small θ_μ values (ranging from 5° to 16°) and large θ_σ values (ranging from ±24° to ±45°). Thus, despite the lack of an exact fit for $\rho = 0.59$ and $r = -0.021$, it is apparent that the heme molecular planes in a cyt *c* film adsorbed to hydrophilic glass are very broadly distributed about a mean tilt angle that is close to the normal axis to the film plane. Consequently, for purposes of comparison to other films, the average values of θ_μ and θ_σ listed in Table 3 have been entered into Table 2. We consider these values, $\theta_\mu = 12°$ and $\theta_\sigma = \pm 33°$, to be representative of the degree of (dis)order in a cyt *c* film adsorbed to hydrophilic glass.

Table 3. Orientation Distributions (deg) Calculated for Selected Combinations of Emission Anisotropy and Dichroic Ratio: Application to Cyt *c* Films on Hydrophilic Glass[a]

dichroic ratio (ρ)	anisotropy (r)				
	−0.001	−0.011	-0.021 ± 0.019[b]	−0.031	−0.041
0.59 ± 0.05[b]	n/o[c]	n/o	n/o	n/o	n/o
0.74	16 ± 24	n/o	n/o	n/o	n/o
0.77	14 ± 29	11 ± 31	10 ± 32	n/o	n/o
0.81	11 ± 34	10 ± 37	5 ± 45	15 ± 31	n/o

[a] Gaussian orientation distributions expressed as $\theta_\mu \pm \theta_\sigma$. [b] Measured ρ and r values (mean ± standard deviation) for cyt *c* adsorbed to hydrophilic glass. [c] Not obtainable (the combination of ρ and r did not produce a simultaneous solution to eqs 1 and 8).

Table 4. Orientation Distributions (deg) Calculated for Selected Combinations of Emission Anisotropy and Dichroic Ratio: Application to Cyt *c* Films on Thiol SAMs[a]

dichroic ratio (ρ)	anisotropy (r)				
	−0.146	−0.161	-0.176 ± 0.030[b]	−0.191	−0.206
1.43	n/o[c]	52 ± 20	61 ± 28	73 ± 38	n/o
1.53	n/o	n/o	52 ± 17	61 ± 26	73 ± 34
1.66 ± 0.23[b]	n/o	n/o	n/o	52 ± 14	61 ± 23
1.79	n/o	n/o	n/o	n/o	52 ± 11
1.89	n/o	n/o	n/o	n/o	n/o

[a] Gaussian orientation distributions expressed as $\theta_\mu \pm \theta_\sigma$. [b] Measured ρ and r values (mean ± standard deviation) for cyt *c* adsorbed to thiol SAM-coated glass. [c] Not obtainable (the combination of ρ and r did not produce a simultaneous solution to eqs 1 and 8).

A similar argument can be made for cyt *c* adsorbed to thiol SAM-coated glass. The orientation distributions calculated from pairs of ρ and r within 1 standard deviation of the respective mean values of 1.66 and −0.176 are shown in Table 4. The orientation distributions listed there have θ_μ values that range from 52° to 73° and θ_σ values ranging from ± 11° to ± 38° (although most θ_σ values are ≥±20°). The average values, $\theta_\mu = 60°$ and $\theta_\sigma = \pm 23°$, are considered representative for the purpose of comparing these samples to protein films adsorbed on other substrates, and appear in Table 2.

The distribution data listed in Table 2 can be separated into two groups: (1) $\theta_\sigma \leq \pm 11°$ for films adsorbed to AA LB films and DDS-coated substrates. In these cases, the distribution is relatively narrow indicating that a relatively high degree of liquid crystalline order is present. The orientation distributions are comparable to the 75° ± 12° measured previously for $DiIC_{18}$-(3) doped into a LB bilayer of AA,[24] and approach that of the Zn-TOPP-doped LB films discussed above. (2) $\theta_\sigma \geq \pm 23°$ for films adsorbed to hydrophilic, thiol SAM-coated, and hydroxy SAMs-coated substrates. In these cases, the distribution is relatively broad, indicating that the films are relatively disordered. The difference between the narrow and broad distributions is illustrated in Figure 6, where normalized Gaussian

(41) (a) Koppenol, W. H.; Margoliash, E. *J. Biol. Chem.* **1982**, *257*, 4426−4437. (b) Sankaram, M. B.; Marsh, D. In *Protein-Lipid Interactions*; Watts, A., Ed.; Elsevier: London, 1993; p 130.

(42) See for example: (a) Pachence, J. M.; Blasie, J. K. *Biophys. J.* **1988**, *52*, 735−747. (b) Heimburg, T.; Marsh, D. *Biophys. J.* **1993**, *65*, 2408−2417 and references therein.

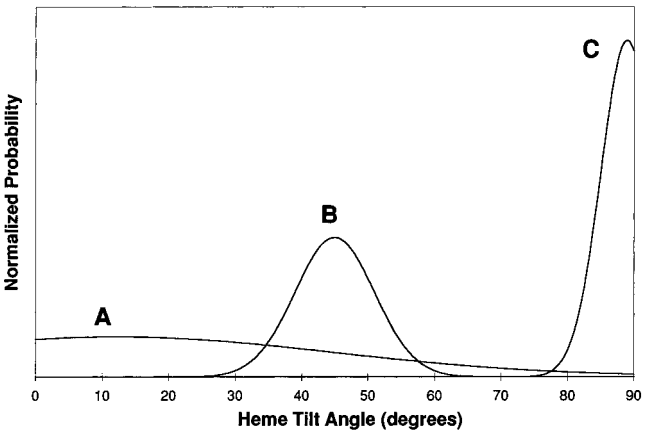

Figure 6. Gaussian probability distributions for (A) cyt *c* adsorbed to hydrophilic glass with $\theta_\mu = 12°$ and $\theta_\sigma = \pm 33°$, (B) cyt *c* adsorbed to on AA LB film with $\theta_\mu = 46°$ and $\theta_\sigma = \pm 6°$, (C) Zn-TOPP doped into a LB bilayer of AA with $\theta_\mu = 89°$ and $\theta_\sigma = \pm 4°$ (these values are representative of the orientation distributions listed in Table 1).

orientation distributions for cyt *c* adsorbed to hydrophilic glass and to AA are plotted. For comparison purposes, the distribution for the Zn-TOPP-doped LB films is also plotted.

The extent of disorder in the second group can be compared to that of FITC-BSA adsorbed to hydrophilic glass, which we examined as a model for a randomly oriented protein film assembly. We reasoned that even if BSA molecules adsorb to glass in a geometrically nonrandom manner, the orientation distribution for the fluorescein label would be relatively isotropic since there is a large number of spatially distributed lysines on the surface of BSA available for attaching a FITC label.

Adsorbed BSA films were prepared by incubating hydrophilic glass substrates with a 38 μM solution of FITC−BSA in phosphate buffer for 30 min, followed by rinsing in phosphate buffer. To prevent energy transfer between surface bound fluorescein moieties, films used in TIRF experiments were prepared from an incubation solution that contained a 10-fold molar excess of unlabeled BSA (i.e., the total protein concentration was 38 μM but the fluorescein concentration was only 2.6 μM). Linear dichroism and anisotropy measurements yielded a mean tilt angle of $63° \pm 2°$ ($n = 2$) and an anisotropy of -0.214 ± 0.009 ($n = 3$), respectively. Using the theory for a linear dipole presented in a previous paper[24] and assuming $\gamma = 0°$, a Gaussian orientation distribution of $63° \pm 30°$ was calculated. These values are reasonably close to the theoretical expectation for a completely random distribution, which is $\theta_\mu = 55°$ and $\theta_\sigma \geq \pm 30°$.[43] More significantly, with reference to the data listed in Table 2, it is apparent that the orientational disorder in cyt *c* films adsorbed on hydrophilic, thiol SAM-coated, and hydroxy SAM-coated substrates is comparable to that in the FITC−BSA film.

The remainder of this section addresses the question, Why is the orientation distribution narrow in some cyt *c* films and broad in others? One probable explanation is that a broad distribution results from multiple types of adsorptive interactions. In other words, adsorption to the substrate occurs via several contact regions on the surface of the protein. These different protein−substrate interactions may share a common physical basis (e.g., all primarily electrostatic) or may be physically distinct (e.g., some primarily electrostatic, some primarily hydrophobic). Regardless, the net result will be a film composed of subpopulations of molecules in different geometric orientations, which will sum to produce a broad orientation distribution (as measured using the IOW-ATR + TIRF method). In contrast, a narrow distribution will be produced when the protein adsorbs to the surface predominately at a single contact region, presumably via a single type of physical interaction of high affinity (relative to competing interactions).

Consequently, a limited investigation into the physical nature of cyt *c* adsorption to DDS-coated glass, hydrophilic glass, and AA LB films was undertaken. Experiments were performed to determine the extent to which cyt *c* could be desorbed from these substrates by soaking them in buffer solutions containing a high salt concentration or a nonionic surfactant. Epifluorescence microscopy of Zn-cyt *c* was used to quantitatively monitor the extent of desorption. The intent was to determine if the (approximately) monolayer films formed by adsorption on these three substrates contained distinct subpopulations of protein molecules.

For these experiments, the substrate was first mounted in a liquid cell. Protein films were formed by adsorption from solutions containing 1:10 Zn-cyt *c*/ferrocyt *c*, under the same conditions used to form films for TIRF anisotropy measurements. After the film was rinsed in 50 mM phosphate buffer (pH 7.2, ionic strength of 113 mM) without being allowed to dry, the cell was refilled with phosphate buffer and the fluorescence emission intensity was measured. The cell was then filled with buffer containing 200 mM KCl (ionic strength of 313 mM). After soaking periods ranging from 15 min to 24 h, the cell was refilled with phosphate buffer and the emission intensity was again measured. In other cases, after the initial rinse in phosphate buffer, the slide was soaked in buffer containing 2% (v/v) Triton X-100 for periods ranging from 15 min to 24 h (i.e., the treatment with 200 mM KCl was bypassed). The results are shown in Table 5. Listed are the emission intensities measured after application of each desorption treatment, normalized to the first value measured for each film after the initial rinse in phosphate buffer.

The data indicate that the nature of cyt *c* binding to hydrophilic glass is complex. Some fraction of the molecules in the film appear to be electrostatically adsorbed, since treatment with high ionic strength buffer for periods of 15 min and 24 h desorbed 16% and 40% of the film, respectively. Treatment with 2% Triton X-100 for 15 min caused 53% of the film to desorb, and extending this treatment to 24 h removed 64%. For the purposes of this discussion, the remaining 36% is considered "irreversibly" adsorbed. The nature of the adsorptive interactions between a protein molecule and a glass surface that both can and cannot be disrupted by Triton X-100 is unknown. However, it is clear from these data that several types of interactions exist between the surfaces of the cyt *c* molecule and hydrophilic glass.

Significantly different behavior was observed for cyt *c* adsorbed to AA LB films. Soaking in high ionic strength buffer for only 15 min removed 47% of the protein; extending this treatment to 24 h removed a total of 91%. These data strongly suggest that a single mechanism, electrostatic attraction, dominates the binding interaction between cyt *c* and arachidic acid LB films. Similar results have been reported for cyt *c* adsorbed to negatively charged membranes and self-assembled monolayers.[5a,42] The predominance of electrostatic adsorption is not surprising given that (i) the charge on the protein at pH 7 is

(43) Note that when $\theta_\mu = 55°$ for a linear dipole, θ_σ is relatively insensitive to differences in r. Thus, anisotropy measurements cannot distinguish between $\theta_\sigma = \pm 30°$ and $\theta_\sigma > 30°$. See Figure 6 in ref 24.

Table 5. Desorption of Zn-cyt *c* from Substrate Surfaces by Salt and Surfactant Solutions

desorption treatment	percentage (%) of initial fluorescence intensity remaining after applying desorption treatments to adsorbed cyt *c* films[a]		
	hydrophilic glass	arachidic acid LB film	DDS-coated glass
50 mM buffer rinse[b]	100	100	100
50 mM buffer containing 200 mM KCl, 15 min static incubation	84 ± 4.5 ($n = 2$)	53 ± 7 ($n = 5$)	94 ± 10 ($n = 3$)
50 mM buffer containing 200 mM KCl, 24 h static incubation	60 ± 4 ($n = 2$)	9 ± 3 ($n = 3$)	55 ± 3 ($n = 2$)
2% Triton X-100 in 50 mM buffer, 15 min static incubation[d]	47 ± 3.5 ($n = 2$)	nm[c]	22 ± 6 ($n = 3$)
2% Triton X-100 in 50 mM buffer, 24 h static incubation[d]	36 ($n = 1$)	nm[c]	8 ± 2 ($n = 3$)

[a] Films were formed by adsorption from solutions containing 1:10 Zn-cyt *c*/ferrocyt *c*, under the same conditions used to form films for orientation distribution measurements (Table 2). Emission intensities measured after application of desorption treatments were normalized to the first value measured for each film after the initial rinse in phosphate buffer. [b] 50 mM phosphate buffer, pH 7.2. [c] Not measured. [d] Desorption experiments using Triton X-100 were performed on protein films that had been rinsed in 50 mM buffer but had not been soaked in 200 mM KCl solution.

+9[41] and (ii) the hydrophilic headgroup plane of an AA LB film should be highly ordered and uniformly charged.[44]

Another type of behavior was observed for cyt *c* adsorbed to DDS-coated glass. Soaking in high ionic strength buffer for 15 min removed only 6% of the protein; extending this treatment to 24 h removed a total of 45%. Treatment with 2% Triton X-100 for periods of 15 min and 24 h removed 78% and 92% of the protein, respectively. These results suggest that a significant fraction of the protein film is weakly bound via electrostatic forces. This is not surprising since it is well known that silanizing a glass surface reduces but does not eliminate its intrinsic negative charge.[45] However, the essentially quantitative removal in 2% Triton X-100 indicates that the adsorption of cyt *c* to DDS-treated glass is predominately hydrophobic in nature, which is expected on the basis of the wettability of the substrate surface (water contact angle of 88°).

Overall, the results of the desorption experiments support the idea that cyt *c* adsorption to either an arachidate LB film or DDS-coated glass is dominated by a single, substrate-specific type of noncovalent interaction, whereas multiple types of interactions occur between cyt *c* and hydrophilic glass. Furthermore, only on hydrophilic glass does irreversibly adsorbed protein comprise a significant fraction of the film. This model correlates well with the orientation distribution data: Narrow distributions result from protein adsorption via a single, dominant interaction, whereas a broad distribution is observed for a protein film generated via multiple types of adsorptive interactions.

In the case of AA LB films, the narrow orientation distribution can be rationalized in terms of the protein structure. It is well known that the distribution of charged residues on the surface of cyt *c* is highly asymmetric.[41] The calculated dipole moment is greater than 300 D, with the dipole vector oriented about 33° from the heme plane.[41a] The asymmetry is readily observable by examining the crystal structure of the protein (we used the program Insight II, Biosym Technologies, San Diego, operating on a Silicon Graphics workstation). Lysine residues are enriched on the protein face where the heme edge is exposed, and carboxylates are located primarily on the top and back of the molecule. Thus, in retrospect, it is not surprising that a narrow orientation distribution is produced when cyt *c* adsorbs to a negatively charged, physically homogeneous substrate.

The physical basis for the narrow distribution of heme tilt angles on DDS-coated substrates is less clear. By analogy to the AA LB film case, a favored interaction between one face on the protein molecule and the substrate surface is indicated. On the basis of the desorption data, this face is predicted to be predominately hydrophobic, although it also may contain positively charged residues (since a considerable fraction of absorbed protein could be desorbed in 200 mM KCl). However, the existence of such a face is not apparent from a qualitative examination of the crystal structure. There is a noticeable lack of hydrophobic residues on those areas of the cyt *c* surface that are locally enriched with charged amino acids, and the distribution of hydrophobic residues over the remainder of the surface appears to be relatively uniform. Thus, in contrast to the AA LB film case, our experimental observation of an oriented cyt *c* film adsorbed to DDS-treated glass is not readily supported on the basis of the crystal structure.

Overall, our data suggest that the adsorptive interaction(s) between the surfaces of the protein and the substrate is the dominant factor governing molecular orientation in adsorbed cyt *c* films. However, other factors may influence the presence of macroscopic (dis)order and should be considered.

First, a conformational change induced by adsorption[1,2] may alter the geometric relationship between the heme plane and the three-dimensional polypeptide matrix surrounding it. Consequently, there are at least three possible explanations for the broad distribution of heme tilt angles in a cyt *c* film adsorbed to hydrophilic glass: (i) The protein is adsorbed via several different contact regions on the surface of the protein, which produces a film containing subpopulations of molecules having different geometric orientations. (ii) The protein adsorbs via a single contact region, but a broad distribution in the extent of adsorption-induced conformational changes produces a broad molecular orientation distribution. (iii) A combination of (i) and (ii). At this point, we cannot distinguish between these possibilities.

Second, lateral interactions between adjacent protein molecules in a closely packed film could be an energetically important factor in producing a macroscopically oriented film at a solid−liquid interface. Lateral interactions coupled with lateral diffusion appear to be necessary to form two-dimensional protein crystals at the air−water interface.[46] In this study, the two films with surface coverages substantially less than a monolayer (on thiol and hydroxy SAMs) were disordered. However, substantial disorder was also present in the film adsorbed on hydrophilic glass, which had a surface coverage greater than one monolayer. Therefore, the presence of adjacent protein molecules in itself does not appear to be a sufficient condition for producing an oriented film. However, it should be noted that we do not know if the extent of lateral interactions differed among the protein films adsorbed to hydrophilic glass, DDS-coated glass, and AA LB films.

Assessment of the Method. The results presented above and in the accompanying paper demonstrate that orientation

(44) Fatty acid LB films have been extensively studied and are known to be well ordered on a macroscopic scale. See: (a) Ulman, A. *An Introduction to Ultrathin OrganicFilms*; Academic: San Diego, 1991. (b) Zasadzinski, J. A.; Viswanathan, R.; Madsen, L.; Garnaes, J.; Schwartz, D. K. *Science* **1994**, *263*, 1726−1733.

(45) See for example: Chen, M; Cassidy, R. M. *J. Chromatogr.* **1992**, *602*, 227−234.

(46) Ahlers, M.; Müller, W.; Reichert, A.; Ringsdorf, H.; Venzmer, J. *Angew. Chem., Int. Ed. Engl.* **1990**, 29, 1269−1285.

distributions in hydrated heme protein films can be measured using the IOW-ATR + TIRF method. This technique is sensitive to submonolayer coverages. Using our existing instrumental arrangement, the sensitivity for linear dichroism measurements is in the range of 5−10% of a monolayer (ca. 10^{-12} mol/cm^2 for cyt *c*) for a chromophore of moderate molar absorptivity (e.g., $\epsilon = 8800$ M^{-1} cm^{-1} at 514.5 nm). A substantially lower detection limit could be achieved if the IOW-ATR measurements were performed at a wavelength near the peak of the Soret absorbance band, where the molar absorptivity is about 10-fold greater. Due to the intrinsic sensitivity of fluorescence and the high throughput of our instrument, steady-state anisotropy measurements can be readily performed on a film of chromophores having moderate photophysical properties ($\epsilon \approx 5000$ M^{-1} cm^{-1} and quantum yield ~0.1) and very low surface coverage (on the order of 10^{-14} mol/cm^2 for a zinc porphyrin). Thus, with respect to sensitivity, the use of the IOW-ATR + TIRF method to examine orientation distributions in molecular films will always be limited by the IOW-ATR measurement.

Finally, as employed here, the method requires the assumption of a functional form for $N(\theta)$. We emphasize that the validity of assuming a Gaussian form for the distribution of heme tilt angles in a molecular film has not been independently verified. More complex models may be more appropriate to describe orientation distributions in other types of molecular assemblies. For example, if a protein is adsorbed via two distinct contact regions that are spatially separated on the surface of the molecule, the actual distribution would be a weighted composite of the two subpopulations. An experimental technique that measures only two variables and assumes a single Gaussian distribution would likely generate results indicating that a broad orientation distribution was present in the film, even if the respective distribution of each subpopulation was quite narrow. However, a unique solution for a distribution function described by more than two independent parameters cannot be obtained using a technique that measures only two variables.

Conclusions

A combination of IOW-ATR linear dichroism and TIRF anisotropy techniques was employed to study molecular orientation in heme protein films. The data presented here and in the accompanying paper are the first orientation distribution measurements reported for protein film assemblies. The results in this paper show that a macroscopically ordered film of adsorbed cyt *c* molecules can be produced when a single, high-affinity type of noncovalent binding occurs between the surface of the protein and the substrate surface. When multiple, competing adsorptive interactions are operative, a relatively disordered film will be produced. Although these findings are not surprising in retrospect, their direct observation is unprecedented. In addition to protein films, the IOW-ATR + TIRF method should prove useful in studying relationships among assembly technique, structure, and function in other types of two-dimensional molecular arrays.

Acknowledgment. We thank Professors Victor Hruby and David O'Brien (University of Arizona) for use of the HF apparatus and the fluorometer, respectively, and Laurie Wood and Sergio Mendes (University of Arizona) for helpful discussions and review of the paper. This work was supported by the National Science Foundation (Grant CHE-9403896) and the National Institutes of Health (Grant R29 GM50299). Acknowledgment is also made to the donors of the Petroleum Research Fund, administered by the American Chemical Society, for partial support of this research.

Supporting Information Available: A more complete description of the experimental procedures used in this work (12 pages). See any current masthead page for ordering and Internet access instructions.

JA962366A